

Published in final edited form as:

Epilepsia. 2012 July ; 53(7): 1205–1214. doi:10.1111/j.1528-1167.2012.03530.x.

Glissandi: transient fast electrocorticographic oscillations of steadily increasing frequency, explained by temporally increasing gap junction conductance

Mark O. Cunningham¹, Anita Roopun¹, Ian S. Schofield², Roger G. Whittaker², Roderick Duncan³, Aline Russell³, Alistair Jenkins⁴, Claire Nicholson⁴, Miles A. Whittington¹, and Roger D. Traub⁵

Mark O. Cunningham: mark.cunningham@ncl.ac.uk; Anita Roopun: anita_roopun@hotmail.com; Ian S. Schofield: ian.schofield@nuth.nhs.uk; Roger G. Whittaker: roger.whittaker@nuth.nhs.uk; Alistair Jenkins: Alistair.Jenkins@nuth.nhs.uk; Claire Nicholson: claire.nicholson@nuth.nhs.uk; Miles A. Whittington: m.a.whittington@newcastle.ac.uk

¹Institute of Neuroscience, The Medical School, Framlington Place, Newcastle University, Newcastle upon Tyne, U.K

²Department of Clinical Neurophysiology, Level 2, New Victoria Wing, Royal Victoria Infirmary, Queen Victoria Road, Newcastle upon Tyne NE1 4LP, U.K

³Department of Clinical Neurophysiology, Institute of Neurological Sciences, Southern General Hospital, Glasgow, U.K

⁴Department of Neurosurgery, Leazes Wing, Royal Victoria Infirmary, Newcastle upon Tyne NE1 4LP, U.K

⁵Department of Physical Sciences, IBM T.J. Watson Research Center, Yorktown Heights, NY 10598, U.S.A.; and Department of Neurology, Columbia University, New York, NY 10032, U.S.A

Abstract

Purpose—We describe a form of very fast oscillation (VFO) in patient electrocorticographic (ECoG) recordings, that can occur prior to ictal events, in which the frequency increases steadily from ~30–40 Hz to >120 Hz, over a period of seconds. We dub these events “glissandi” and describe a possible model for them.

Methods—Four patients with epilepsy had presurgical evaluations (with ECoG obtained in two of them), and excised tissue was studied *in vitro*, from 3 of the patients. Glissandi were seen spontaneously *in vitro*, associated with ictal events; using acute slices of rat neocortex; and they were simulated using a network model of 15,000 detailed layer V pyramidal neurons, coupled by gap junctions.

Key findings—Glissandi were observed to arise from human temporal neocortex. *In vitro*, they lasted 0.2 to 4.1 seconds, prior to ictal onset. Similar events were observed in the rat *in vitro*, in layer V of frontal neocortex, when alkaline solution was pressure-ejected; glissandi persisted when GABA_A, GABA_B, and NMDA and AMPA receptors were blocked. Non-alkaline conditions, prevented glissando generation. In network simulations, it was found that steadily increasing gap junction conductance would lead to the observed steady increase in VFO field frequency. This

Address for correspondence: Dr. Traub at IBM address (5), rtraub@us.ibm.com, 1-914-945-2110.

We confirm that we have read the Journal’s position on issues involved in ethical publication and affirm that this report is consistent with those guidelines.

Disclosure: The authors have no conflicts of interest to report.

occurred because increasing gap junction conductance shortened the time required for an action potential to cross from cell to cell.

Significance—The *in vitro* and modeling data are consistent with the hypothesis that glissandi arise when pyramidal cell gap junction conductances rise over time, possibly as a result of an alkaline fluctuation in brain pH.

Keywords

very fast oscillations; electrocorticography; gap junction; pH; epilepsy model

Very fast oscillations (VFO, >70–80 Hz up to ~250 Hz – we do not consider “fast ripples” here) can be generated by networks of hippocampal and pyramidal neurons, under conditions of blockade of chemical synapses, with the generation and synchronization dependent upon electrical coupling via gap junctions (Draguhn et al., 1998; Nimrich et al., 2005; Traub et al., 2003; Traub et al., 2010; reviewed in Traub & Whittington, 2010). The requisite electrical coupling is most likely through the axons, because of the apparent requirement for action potentials to cross from cell to cell in order to produce the oscillation (Traub et al., 1999, 2003; Schmitz et al., 2001; Hamzei-Sichani et al., 2007). VFO of this sort can be sustained for seconds (Traub et al., 2010).

VFO mechanisms are important to understand for clinical reasons: runs of VFO may occur prior to seizures, both focal and generalized in patients, as well as serving as a biomarker for seizure onset when VFO is isolated; and additionally, VFO occurs in many experimental epilepsy models (Akiyama et al., 2006; Bragin et al., 1999; Fisher et al., 1992; Grenier et al., 2003; Jacobs et al., 2008; Khosravani et al., 2009; Kobayashi et al., 2004; Roopun et al., 2009; Schevon et al., 2008; Traub et al., 2001, 2010; Worrell et al., 2004; and many other authors).

In this paper, we shall use the term “glissando”, a musical term referring to a sequence of notes – such as would be produced by running the fingers across the strings of a harp – notes that are of steadily rising pitch. VFO “glissandi” occur in ECoG recordings in at least some epilepsy patients, just prior to seizures, with frequencies starting in beta/gamma range (tens of Hz), and rising gradually to over 100 Hz. Glissandi can also be observed in experimental *in vitro* conditions, with human or rodent neocortical tissue, under baseline conditions but especially when the extracellular medium is made alkaline; chemical synaptic transmission is not necessary. Using simulations, we show that the axonal crossing time (the time it takes for a spike in one axon to evoke a spike in an electrically coupled axon) is expected to change with gap junction conductance: a parameter that is pH sensitive. As a result, in simulations as in *in vitro* experiments and in patients, a characteristic VFO of increasing frequency can be generated, from a few tens of Hz to well over 100 Hz. Because of the sensitivity of gap junction conductances (Spray et al., 1981), and of VFO itself (Draguhn et al., 1998), to pH, our data suggest that rising brain pH may be a factor in the initiation of epileptic seizures. This is consistent with other recent *in vivo* and clinical observations (Helmy et al., 2011; Schuchmann et al., 2006, 2011; Tolner et al., 2011).

Methods

Patient recordings and tissue

Patient “B”, whose ECoG data are shown in Figure 1, is Patient B from Roopun et al. (2009), with patient details reported therein.

Data from slice studies were derived from three additional patients with medically intractable temporal lobe epilepsy undergoing elective neurosurgical tissue resection. All

patients gave their informed consent, before surgery, for the use of the resected brain tissue. This study was approved by the County Durham & Tees Valley 1 Local Research Ethics Committee (06/Q1003/51) (date of review 03/07/06), and had clinical governance approved by the Newcastle Upon Tyne Hospitals NHS Trust (CM/PB/3707). Details on these three patients are as follows:

Patient 1 was a 56-year old man with a history of epilepsy from the age of 10 years. His epilepsy took the form of complex partial seizures with automatisms (5–10 per month), drop attacks (3–4 per annum) and secondary generalization (<1 per annum). The patient's medication consisted of levetiracetam, carbamazepine, phenytoin, pregabalin and lamotrigine. EEG recordings revealed an active left temporal lobe focus with MRI investigations demonstrating a cavernoma posterior and inferior to the motor strip. Following surgery to remove the cavernoma, the patient has been seizure free. *In vitro* recordings were conducted in slices of inferior temporal gyrus.

Patient 2 was a 29-year old woman with congenital right hemiparesis who has had a history of seizures from the age of 3 years. The patient experiences 2–3 seizures per day and these are associated with foul taste in the mouth, oral automatisms, coughing and belching. The patient has also experienced one episode of status epilepticus at the age of 10 years. The patient's medication consisted of valproate, carbamazepine, topiramate, pregabalin and clonazepam. EEG recordings revealed a left temporal slow wave discharge and MRI investigations showed left hippocampal sclerosis with porencephaly in the left parietal region. Her SPECT study was significantly abnormal, showing hypoperfusion in the left temporoparietal region. A selective amygdalo-hippocampectomy was carried out and the patient was then seizure-free for 3 years; however, seizures have recurred with same semiology as described above. *In vitro* recordings were conducted in slices of inferior temporal gyrus.

Patient 3 was a 49-year old woman with a history of seizures from the age of 31 years. These events, which occur approximately 1 per month, are associated with epigastric sensations, agitation and loss of consciousness. The patient's medication consisted of valproate, carbamazepine and lamotrigine. EEG recordings revealed sharp waves in the right temporal lobe and MRI investigations demonstrated a right temporal pole lesion. A right anterior temporal lobectomy was conducted and subsequent histological analysis demonstrated that the lesion was a Grade II astrocytoma. ECoG was obtained perioperatively. The patient has had 3 seizures per month post-operatively. *In vitro* recordings were conducted in slices of posterior superior temporal gyrus.

In vitro human neocortex recordings—Human slices were derived from material removed as part of surgical treatment of medically intractable cortical epilepsy from the left and right temporal regions with written informed consent of the patients. Anesthesia was induced with intravenous remifentanyl with/without alfentanil (0.2–0.4 µg/kg, 1 mg/kg, respectively). At induction a bolus dose of propofol (1–2 mg/kg) was administered intravenously. The patient also received a muscle relaxant, vecuronium (0.1 mg/kg). Anesthesia was maintained with remifentanyl, oxygen, and desflurane at minimum alveolar concentration (MAC) volume of 0.5–1. Resected tissue was immediately transferred to sucrose-containing artificial cerebrospinal fluid (sACSF) containing (mM): 252 sucrose, 3 KCl, 1.25 NaH₂PO₄, 2 MgSO₄, 2 CaCl₂, 24 NaHCO₃ and 10 glucose. Neocortical slices containing all layers were cut at 450 µm (Microm HM 650 V), incubated at room temperature for 20–30 min, then transferred to a standard interface recording chamber at 34–36°C perfused with oxygenated ACSF containing (mM): 126 NaCl, 3 KCl, 1.25 NaH₂PO₄, 1 MgSO₄, 1.2 CaCl₂, 24 NaHCO₃ and 10 glucose. The time between resection and slice preparation was <1 min. Extracellular recordings (DC–500 Hz) were conducted with ACSF-

filled glass microelectrodes (2 M Ω) connected to an extracellular amplifier (EXT-10-2F, npi electronic GmbH, Tamm, Germany).

In vitro rat neocortex recordings—450 μm thick horizontal slices were prepared from adult male Wistar rats (150–250 g). Neocortical slices containing frontal and/or temporal association areas were maintained at 34°C at the interface between warm wetted 95% O₂/5% CO₂ and ACSF containing (in mM): 3 KCL, 1.25 NaH₂PO₄, 1 MgSO₄, 1.2 CaCl₂, 24 NaHCO₃, 10 glucose and 126 NaCl. Extracellular recordings from layer V were obtained using glass micropipettes containing the above ACSF (resistance < 0.5 M Ω). Signals were analog filtered at 1 Hz – 2 kHz and digitized at 10 kHz. Epileptiform events were evoked by pressure ejection of 30–70 nl ACSF containing 100–200 mM NaOH (pH 8.2–8.9) onto layer 5. Droplets were placed in layer V, approximately 100 – 300 μm from the recording site (also in layer V). [Application directly onto the recording site did not generate glissandi, perhaps because of a lack of time-dependence of local pH changes.] The main chemical synaptic pathways were blocked by bath application of NBQX (20 μM), D-AP5 (50 μM), gabazine (1 μM) and CGP55845 (10 μM) [respectively blocking AMPA, NMDA, GABA_A, GABA_B receptors], all obtained from Tocris, UK. For control experiments, BAPTA (1,2-bis(o-aminophenoxy)ethane-N,N,N',N'-tetraacetic acid) was purchased from Sigma, UK.

Detailed multicompartiment neuronal models—The methods used are similar to those described in Traub et al. (2010), with some variations described below. Briefly, we used a model of a layer V tufted pyramidal cell similar to the 61-compartment one described in Traub et al. (2005). The major difference was that the transient (“A”) K⁺ current was increased in the axon, approximately following data of Shu et al. (2007). [The current described by Shu et al. (2007) is slowly inactivating, whereas the current we used inactivated rapidly; this, however, was not important for our purposes.] For the sake of simplicity, we blocked high-threshold g_{Ca} and slow after hyperpolarization currents, suppressing the tendency of the cells to generate intrinsic bursts.

We ran simulations of single neurons and of large populations. Single neuron simulations were used to study the effect of gap junction conductance on the transmission of a spike from one axon to another. This was done by injecting current into the distal axon, as would occur if a spike in a coupled axon was occurring and was coupled to the simulated cell through a conductance; this latter conductance was then varied as a parameter. For network simulations, we used 15,000 model neurons, electrically coupled through gap junctions between distal axonal compartments, in a random network topology. [Based on analysis of the behavior of simplified network models (Vladimirov et al., 2011), we believe that the details of the topology are not critical for the results reported here.] There were an average of 3.333 gap junctions on each axon. In the network simulations, there were two parameters studied: the gap junction conductance, assumed to be equal at all gap junctions in the network; and the density of the “M” type of K⁺ conductance: a non-inactivating type of K⁺ conductance that is activated by depolarization, that relaxes with a time constant in the tens of ms at potentials near the resting potential, and that is present in the axon as well as soma and dendrites (Pan et al., 2006). We varied g_{K(M)} in a systematic way, as follows: we started with a baseline density of the conductance in different compartments (30 mS/cm² on the axon, 11.9 mS/cm² on the soma, 19.0 mS/cm² on the apical shaft, oblique and basilar dendrites, and 5.6 mS/cm² in the tuft), a distribution arrived at by multiple trial-and-error simulations, and not assumed to be uniquely capable of replicating experimental traces. We then used a “scaling parameter”, from 0 to 3.5, that multiplied the baseline conductance density in each compartment. We also systematically varied gap junction conductances. Chemical synapses were not simulated.

Simulations of the 15,000 cell network were run on 40 processors of an IBM e1350 Linux cluster and on 20 processors of an IBM 7040-681 AIX parallel computer. Code for the models is available from rtraub@us.ibm.com.

A random network topology was used in the detailed simulations for the following reason: in order to demonstrate best the effects of localized network connectivity, very large networks are required, with hundreds of thousands of cells (Traub et al., 2010); it was not considered practical to simulate such large networks using detailed model neurons. Networks of 15,000 “realistic” neurons are large enough to study frequency effects of parameter variations, but not spatial properties. The physical point that this paper seeks to demonstrate – that there is a basic time scale determined by gap junction conductance – should hold true in any network topology, however.

Results

Glissandi can occur in electrocorticographic (ECoG) recordings from human epileptic brain in situ, prior to a seizure

An example of a pre-ictal glissando, in a human ECoG recording, is shown in Figure 1. As seen in Figure 1A, there are large, slow, baseline fluctuations (marked by the horizontal bar) before the electrographic seizure. A glissando discharge is unmasked by removal of the slow baseline fluctuation with a higher pass band filter (lower trace). As seen in Figure 1B, using a sliding window spectrogram, the glissando lasts about 4 seconds, and runs from ~30 Hz to ~125 Hz. An additional spontaneous glissando, similar to that shown in Figure 1, was also observed in the 9 hours of overnight ECoG recording analyzed.

Glissandi occur in excised human epileptic neocortex, as spontaneous events in vitro

Field potential glissandi were observed to arise from human epileptic temporal neocortex in vitro (n=3 patients; n=70 events), lasting 0.2 to 4.1 seconds, with a duration of (mean \pm s.e.m) 0.8 ± 0.1 seconds, and with an average amplitude of 1.7 ± 0.1 mV. The mean initiation frequency of the glissandi was 37.9 ± 1.4 Hz and the glissando had a mean termination frequency of 121.5 ± 3.6 Hz.

Glissandi can be evoked in “normal” rat neocortical slices in alkaline conditions, and also when AMPA, NMDA and GABA receptors are blocked

Transient, spatially localized alkalization of layer V in adult rat neocortex generated ictal events lasting >30s (Figure 3A). The initial field potential event in each case was a low-amplitude ($64 \pm 12 \mu\text{V}$) run of fast oscillations beginning 0.7 ± 0.3 s post application of alkaline solution. The initial peak frequency of this activity was 32 ± 7 Hz. The maximum frequency shifted to 180 ± 30 Hz over 0.5 – 2.2 s until onset of large amplitude ictal events (Figure 3B, $P < 0.05$, n=5). Bathing slices in ACSF containing drugs to block AMPA, NMDA and GABA_A & B receptors abolished the ictal response to alkalization in all cases; however, the initial, low amplitude fast oscillation persisted, lasting 0.6 ± 0.2 s with frequency increasing from 44 ± 8 Hz to 220 ± 30 Hz (Figure 3B), and latency from droplet application of 0.5 ± 0.2 s (n=5). These initial fast oscillations resembled the glissando discharges seen in human cortex *in vivo* and *in vitro* suggesting that non-chemical intercellular transmission may play a role, and that chemical synapses are not required.

The production of a pro-epileptogenic low calcium environment (Haas and Jefferys, 1984) through alkalization and subsequent precipitation of calcium ions out of the ACSF solution may, in principle, be a factor in the production of the glissandi. In order to address this issue, the fast calcium buffer, BAPTA (1 mM) was pressure ejected in the presence of the cocktail of chemical synaptic antagonists (for AMPA, NMDA, GABA_A and GABA_B

receptors). Following the brief application of BAPTA, no glissandi were observed ($n=3$, data not shown).

The latency for a spike to cross from axon to axon is expected to depend on gap junction conductance—Furshpan and Potter (1959) showed, by direct dual recording from coupled axons, that a spike could cross from one axon to the electrically coupled other axon in <0.5 ms; this was in an invertebrate preparation (the isolated crayfish nerve cord) at room temperature. MacVicar and Dudek (1982) provided indirect evidence that spikes might cross from one hippocampal mossy fiber to another in about 0.2 ms (the reasoning behind this interpretation of their data is in Traub et al. (1999)). Mercer et al. (2006) recorded simultaneously from two CA1 pyramidal cell somata, and demonstrated that a spike in one cell could induce a spikelet in the other cell with latency about 0.5 ms; if the coupling is mediated between axons (which was not proven in the paper), then – allowing for conduction times – the axonal crossing time must be less than 0.5 ms. Dhillon and Jones (2000) demonstrated a similar phenomenon in entorhinal cortex. Wang et al. (2010) recorded simultaneously from two layer V pyramidal neurons, and reported spike/spikelet latencies of 0.18 to 1.8 ms. We are not aware of experimental data examining spike latencies that are modified by manipulations of gap junction conductance, and therefore examined this question with simulations (Figure 4).

In order to construct Figure 4, we first determined the waveform, $V(t)$, of a simulated axonal action potential, over a time interval of 1.0 ms. We then simulated a current-induced spike, and injected, starting at time 10 ms (arrow in Figure 4), the current $g \times V(t)$ into the distal axonal compartment, where g represents the putative gap junction conductance. We repeated this procedure for $g = 1, 2, 3, \dots, 10$ nS. The resulting axonal responses are shown, superimposed, in Figure 4, and are taken to represent the properties of axon-axon spike transmission as a function of gap junction conductance. [The data in Figure 4 do not, however, capture the effects of shunting when multiple nearby gap junctions are present on an axon.] Figure 4 shows clearly that, as expected, once a threshold conductance is reached, the latency for spike transfer diminishes as the coupling conductance increases – with “diminishing returns”, however, at larger conductances. The difference in latency to the peak of the spike, from $g = 3$ nS to 4 nS, is 0.08 ms; the difference in latency from $g = 3$ nS to 10 nS, is 0.18 ms.

We repeated the simulations of Figure 4, injecting currents in progressively more proximal axonal compartments, rather than the most distal one (not shown). Using the penultimate axonal compartment produced results similar to Figure 4; however, with the next, more proximal, compartment, the spread in latencies became larger, almost 1 ms. This might suggest a larger spread in glissando frequencies, but see further on.

The functional significance of these latency differences, for network behavior, can be estimated as follows: in a VFO network modeled as a random graph, oscillation periods are expected to follow the mean path length, being of order twice this quantity (Traub et al., 1999) [The “mean path length”, for a connected subregion of a graph, is the average number of steps it takes to traverse a shortest path from node 1 to node 2, where both nodes are chosen randomly. In a random graph with sufficiently high connectivity, there is a single connected subregion that is much larger than all the others, called the “large cluster”. Comments below refer to the large cluster.] In a random graph, the statistical structure is determined entirely by the connectivity parameter c [equal to $\frac{1}{2}$ the mean number of edges, or links, emanating from a node – the “mean index”]; c in turn determines the relative size of the large cluster in the graph, $G(c)$, a number lying between 0 and 1 (Erdős and Rényi, 1960). In our case, where the mean index of the 15,000 cell random graph is 3.333, c is

equal to half of this, or about 1.667, and $G(c) = 0.96$. That is, the large cluster is 96% of the whole network. Following Newman et al. (2001), we may estimate the mean path length as

$$\sim 1 + \log(N \times G(c)/2c) \log(2c),$$

where N is the graph size, or 15,000. This quantity is about 8.0. Thus, a difference in latency of 0.18 ms for a spike to cross from axon to axon (see above) is expected to translate into differences in VFO periods of the order of $2 \times 8 \times 0.18 \text{ ms} \sim 2.9 \text{ ms}$. That number is sufficient to make a major difference in network frequency. Thus, if the fastest VFO frequency in the network were, say, 160 Hz, corresponding to a period of 6.25 ms, then the network might be capable of slowing down to a period of $6.25 + 2.9 = 9.15 \text{ ms}$, or a frequency of 109 Hz. Simulations (see below) and experiments (see above) indicate that networks can oscillate at even lower frequencies than this. Because the above analysis does not take into account the effects of shunting caused by multiple gap junctions, and by multiple axonal K^+ conductances, we can not expect it to account for the extremes of the network frequency range.

Glissandi are predicted to occur, in a detailed network model, as gap junction conductance increases, provided $g_{K(M)}$ is sufficiently large—In order to study the effects of gap junction conductance on VFO frequency in detailed network simulations (see Methods), we performed a large number of 1-second simulations as this parameter was varied, along with a parameter scaling $g_{K(M)}$, the density of the M-type of K^+ conductance (Figure 5A). Chemical synaptic conductances were not simulated. We found that VFO frequency would indeed steadily rise as gap junction conductance increased – predicting the existence of a glissando – provided that $g_{K(M)}$ was large enough. In Figure 5A, the scaling parameter for $g_{K(M)}$ needed to be ~ 1.5 or larger for a glissando to be expected.

Figure 5B provides a more detailed view of network behavior, at a fixed $g_{K(M)}$ value (scaling factor 2.7, see Figure 5A), for two specific values of gap junction conductance. The model predicts that spikelet frequency (in intracellular recordings) should increase as network frequency increases (compare Fig. 10.7 of Traub & Whittington, 2010).

Another parameter that influences network frequency under the conditions of Figure 5 is axonal $g_{K(A)}$. Reductions of the density of this transient K^+ conductance, approximately 4-fold compared to Figure 5, could lead to network frequencies approaching 300 Hz (not shown).

The network model replicates full glissandi, when gap junction conductance is increased over time, and over an appropriate range

In the simulation of Figure 6, the $g_{K(M)}$ scaling factor was also 2.7 (c.f. Figure 5), and gap junction conductance was increased from 2.0 to 12.0 nS, over a period of 2 seconds. Chemical synaptic conductances were not included in the simulation. The glissando thereby produced was strikingly similar to the examples recorded from patients and in vitro slices in “non-synaptic” conditions. We repeated this simulation (not shown) with gap junctions located in more proximal compartments, rather than the most distal axon. Using the penultimate axon compartment led to a glissando similar to that shown in Figure 6. Moving the gap junctions one more compartment proximally, however, and leaving all other parameters unchanged, led to a simulated field without oscillations. This can be attributed to failures of spike transmission across gap junctions, due to the impedance load of the soma and dendrites.

Discussion

We have shown that “glissandi” – field oscillations of steadily increasing frequency, from tens of Hz evolving to over 100 Hz – occur spontaneously in human epileptic neocortical tissue. Experimentally, glissandi are favored by blockade of chemical synapses and by alkalization of the tissue; however, blockade of chemical synapses does not appear to be essential (Figure 3).

Glissandi can plausibly be explained by progressively opening gap junctions between principal neurons (Figure 6). The essential physical idea is that altering gap junction conductance should modify the propagation time for a spike to pass from cell to cell, independent of the details of membrane kinetics. Other factors, however, that could increase VFO frequency can not yet be definitively ruled out. Examples of such other factors would include increasing axonal excitability and increased rates of spontaneous firing in the axonal plexus (Traub et al., 1999, 2010; Lewis and Rinzel, 2000).

The occurrence of glissandi prior to seizures, as a proposed consequence of opening gap junctions, is consistent with suggestions that brain alkalization, perhaps induced by hyperventilation, contributes to seizure initiation in certain clinical and experimental contexts (Schuchmann et al., 2006, 2011); and alkalization could explain why acetazolamide is effective in at least some epilepsy patients. We would like to suggest that (possibly localized) brain alkalization could contribute to the initiation of focal seizures (Figure 3, and Traub et al., (2010)), and that alkalization is effective – at least in part – because of its effects on gap junctions between principal neurons. How might such proposals be tested?

First of all, it may be possible to measure brain pH in experimental animals that experience spontaneous seizures (Javaheri et al., 1981). Such studies could, at least in principle, establish a temporal correlation between tissue alkalization and seizure initiation. That alkalization occurs in epileptic temporal lobe has been previously suggested (Laxer et al., 1992), although the detailed time relations between pH changes and seizures was not determined. Even if an appropriate temporal correlation does exist, however, how can one be sure that the relevant physiological effect is an opening of putative axonal gap junctions, and not a change in one or more other biological parameters? This is a particularly troubling question given that a) some axonal gap junctions (in hippocampal mossy fibers) appear to contain connexin36 (Hamzei-Sichani et al., 2007); b) VFO in non-synaptic conditions is enhanced by alkalization (Draguhn et al., 1998); but c) connexin36-containing gap junction channels appear to be closed – not opened – by alkalization (González-Nieto et al., 2008). Additionally, low-calcium induced VFO in hippocampal slices appears identical in control mice as compared to connexin36 knockout mice (Hormuzdi et al., 2001). One must *not* assume, then, that putative axonal gap junctions contain connexin36 as their sole or major component. We would hypothesize that the putative axonal connexin, whatever it turns out to be, is opened by alkalization.

We suggest that molecular techniques are required to unravel these questions. First, it is essential to identify which protein (or proteins) are the most important ones in putative gap junctions between principal neurons. (For example, connexin57 has been shown to mediate axo-axonal coupling in retina (Janssen-Bienhold et al., 2009). Second, it might be possible to genetically engineer this protein so as to render it more, or less, susceptible to conductance changes induced by pH alterations. Third, animals with the suitably engineered gap junction protein may be more, or less, susceptible to epileptogenesis in experimental protocols. Finally, identification of the critical protein should allow preparation of a specific

antibody, which in turn would allow analyses of protein expression in epileptic vs. non-epileptic human tissue.

Acknowledgments

Supported by NIH/NINDS (RO1NS044133 to RDT), IBM (RDT), the Alexander von Humboldt Stiftung (RDT), the Einstein Stiftung Berlin (RDT), the MRC Milstein Fund (U.K.), The Wolfson Foundation, The Royal Society and the Newcastle upon Tyne Healthcare Charities Trust. MC is funded by the Dr Hadwen Trust and did not participate in experiments involving animals or cells or tissues from animals or from human embryos. The content is solely the responsibility of the authors and does not necessarily reflect the official views of the National Institutes of Health or the National Institute of Neurological Disorders and Stroke. We thank Drs. Yuhai Tu, Nikita Vladimirov, Erin Munro, Mark Kramer, and Geoffrey Grinstein for helpful discussions.

References

- Akiyama T, Otsubo H, Ochi A, Galicia EZ, Weiss SK, Donner EJ, Rutka JT, Snead OC III. Topographic movie of ictal high-frequency oscillations on the brain surface using subdural EEG in neocortical epilepsy. *Epilepsia*. 2006; 47:1953–1957. [PubMed: 17116039]
- Bragin A, Engel J Jr, Wilson CL, Fried I, Buzsáki G. High-frequency oscillations in the human brain. *Hippocampus*. 1999; 9:137–142. [PubMed: 10226774]
- Dhillon A, Jones RS. Laminar differences in recurrent excitatory transmission in the rat entorhinal cortex *in vitro*. *Neuroscience*. 2000; 99:413–22. [PubMed: 11029534]
- Draguhn A, Traub RD, Schmitz D, Jefferys JGR. Electrical coupling underlies high-frequency oscillations in the hippocampus *in vitro*. *Nature*. 1998; 394:189–192. [PubMed: 9671303]
- Erdős P, Rényi A. On the evolution of random graphs. *Publ Math Instit Hungar Acad Sci*. 1960; 5:17–61.
- Fisher RS, Webber WRS, Lesser RP, Arroyo S, Uematsu S. High-frequency EEG activity at the start of seizures. *J Clin Neurophysiol*. 1992; 9:441–448. [PubMed: 1517412]
- Furshpan EJ, Potter DD. Transmission at the giant motor synapses of the crayfish. *J Physiol*. 1959; 145:289–325. [PubMed: 13642302]
- González-Nieto D, Gómez-Hernández JM, Larrosa B, Gutiérrez C, Muñoz MD, Fasciani I, O'Brien J, Zappalà A, Cicirata F, Barrio LC. Regulation of neuronal connexin-36 channels by pH. *Proc Natl Acad Sci USA*. 2008; 105:17169–17174. [PubMed: 18957549]
- Grenier F, Timofeev I, Steriade M. Neocortical very fast oscillations (ripples, 80–200 Hz) during seizures: intracellular correlates. *J Neurophysiol*. 2003; 89:841–852. [PubMed: 12574462]
- Hamzei-Sichani F, Kamasawa N, Janssen WGM, Yasamura T, Davidson KGV, Hof PR, Wearne SL, Stewart MG, Young SR, Whittington MA, Rash JE, Traub RD. Gap junctions on hippocampal mossy fiber axons demonstrated by thin-section electron microscopy and freeze-fracture replica immunogold labeling. *Proc Natl Acad Sci USA*. 2007; 104:12548–12553. [PubMed: 17640909]
- Haas HL, Jefferys JGR. Low-calcium field burst discharges of CA1 pyramidal neurones in rat hippocampal slices. *J Physiol*. 1984; 354:185–201. [PubMed: 6481633]
- Helmy MM, Tolner EA, Vanhatalo S, Voipio J, Kaila K. Brain alkalosis causes birth asphyxia seizures, suggesting therapeutic strategy. *Ann Neurol*. 2011; 69:493–500. [PubMed: 21337602]
- Hormuzdi SG, Pais I, LeBeau FEN, Towers SK, Rozov A, Buhl EH, Whittington MA, Monyer H. Impaired electrical signaling disrupts gamma frequency oscillations in connexin 36-deficient mice. *Neuron*. 2001; 31:487–495. [PubMed: 11516404]
- Jacobs J, LeVan P, Chander R, Hall J, Dubeau F, Gotman J. Interictal high-frequency oscillations (80–500 Hz) are an indicator of seizure onset areas independent of spikes in the human epileptic brain. *Epilepsia*. 2008; 49:1893–1907. [PubMed: 18479382]
- Janssen-Bienhold U, Trümpler J, Hilgen G, Schultz K, Müller LP, Sonntag S, Dedek K, Kirks P, Willecke K, Weiler R. Connexin57 is expressed in dendro-dendritic and axo-axonal gap junctions of mouse horizontal cells and its distribution is modulated by light. *J Comp Neurol*. 2009; 513:363–374. [PubMed: 19177557]
- Javaheri S, Clendening A, Papadakis N, Brody JS. Changes in brain surface pH during acute isocapnic metabolic acidosis and alkalosis. *J Appl Physiol*. 1981; 51:276–281. [PubMed: 7263434]

- Khosravani H, Mehrotra N, Rigby M, Hader WJ, Pinnegar CR, Pillay N, Wiebe S, Federico P. Spatial localization and time-dependent changes of electrographic high frequency oscillations in human temporal lobe epilepsy. *Epilepsia*. 2009; 50:605–616. [PubMed: 18717704]
- Kobayashi K, Oka M, Akiyama T, Inoue T, Abiru K, Ogino T, Yoshinaga H, Ohtsuka Y, Oka E. Very fast rhythmic activity on scalp EEG associated with epileptic spasms. *Epilepsia*. 2004; 45:488–496. [PubMed: 15101830]
- Laxer KD, Hubsch B, Sappey-Marini D, Weiner MW. Increased pH and inorganic phosphate in temporal seizure foci demonstrated by [³¹P]MRS. *Epilepsia*. 1992; 33:618–623. [PubMed: 1628574]
- Lewis TJ, Rinzel J. Self-organized synchronous oscillations in a network of excitable cells coupled by gap junctions. *Network: Comput Neural Syst*. 2000; 11:299–320.
- MacVicar BA, Dudek FE. Electrotonic coupling between granule cells of the rat dentate gyrus: physiological and anatomical evidence. *J Neurophysiol*. 1982; 47:579–592. [PubMed: 7069454]
- Mercer A, Bannister AP, Thomson AM. Electrical coupling between pyramidal cells in adult cortical regions. *Brain Cell Biol*. 2006; 35:13–27. [PubMed: 17940910]
- Newman MEJ, Strogatz SH, Watts DJ. Random graphs with arbitrary degree distributions and their applications. *Phys Rev E*. 2001; 64:026118.
- Nimmrich V, Maier N, Schmitz D, Draguhn A. Induced sharp wave-ripple complexes in the absence of synaptic inhibition in mouse hippocampal slices. *J Physiol*. 2005; 563:663–670. [PubMed: 15661820]
- Pan Z, Kao T, Horvath Z, Lemos J, Sul JY, Cranston SD, Bennett V, Scherer SS, Cooper EC. A common ankyrin-G-based mechanism retains KCNQ and Na_v channels at electrically active domains of the axon. *J Neurosci*. 2006; 26:2599–2613. [PubMed: 16525039]
- Roopun A, Middleton SJ, Cunningham MO, LeBeau FEN, Bibbig A, Whittington MA, Traub RD. A beta2-frequency (20–30 Hz) oscillation in non-synaptic networks of somatosensory cortex. *Proc Natl Acad Sci USA*. 2006; 103:15646–15650. [PubMed: 17030821]
- Roopun AK, Traub RD, Baldeweg T, Cunningham MO, Whittaker RG, Trevelyan A, Duncan R, Russell AJC, Whittington MA. Detecting seizure origin using basic, multiscale population dynamic measures: Preliminary findings. *Epilepsy Behav*. 2009; 14(Suppl 1):39–46. [PubMed: 18834957]
- Roopun AK, Somonotto JD, Pierce ML, Jenkins A, Schofield I, Kaiser M, Whittington MA, Traub RD, Cunningham MO. A non-synaptic mechanism underlying interictal discharges in human epileptic neocortex. *Proc Natl Acad Sci USA*. 2010; 107:338–343. [PubMed: 19966298]
- Schevon CA, Ng SK, Cappell J, Goodman RR, McKhann G Jr, Waziri A, Branner A, Sosunov A, Schroeder CE, Emerson RG. Microphysiology of epileptiform activity in human neocortex. *J Clin Neurophysiol*. 2008; 25:321–330. [PubMed: 18997628]
- Schmitz D, Schuchmann S, Fisahn A, Draguhn A, Buhl EH, Petrasch-Parwez RE, Dermietzel R, Heinemann U, Traub RD. Axo-axonal coupling: a novel mechanism for ultrafast neuronal communication. *Neuron*. 2001; 31:831–840. [PubMed: 11567620]
- Schuchmann S, Schmitz D, Rivera C, Vanhatalo S, Salmen B, Mackie K, Sipilä ST, Voipio J, Kaila K. Experimental febrile seizures are precipitated by a hyperthermia-induced respiratory alkalosis. *Nature Medicine*. 2006; 12:817–823.
- Schuchmann S, Hauck S, Henning S, Grüters-Kieslich A, Vanhatalo S, Schmitz D, Kaila K. Respiratory alkalosis in children with febrile seizures. *Epilepsia*. 2011; 52:1949–1955. [PubMed: 21910730]
- Shu Y, Yu Y, Yang J, McCormick DA. Selective control of cortical axonal spikes by a slowly inactivating K⁺ current. *Proc Natl Acad Sci USA*. 2007; 104:11453–11458. [PubMed: 17581873]
- Spray DC, Harris AL, Bennett MVL. Gap junctional conductance is a simple and sensitive function of intracellular pH. *Science*. 1981; 211:712–715. [PubMed: 6779379]
- Tolner EA, Hochman DW, Hassinen P, Otáhal J, Gaily E, Haglund MM, Kubová H, Schuchmann S, Vanhatalo S, Kaila K. Five percent CO₂ is a potent, fast-acting inhalation anticonvulsant. *Epilepsia*. 2011; 52:104–114. [PubMed: 20887367]
- Traub, RD.; Whittington, MA. *Cortical oscillations in health and disease*. Oxford University Press; New York, NY: 2010.

- Traub RD, Schmitz D, Jefferys JGR, Draguhn A. High-frequency population oscillations are predicted to occur in hippocampal pyramidal neuronal networks interconnected by axoaxonal gap junctions. *Neuroscience*. 1999; 92:407–426. [PubMed: 10408594]
- Traub RD, Whittington MA, Buhl EH, LeBeau FEN, Bibbig A, Boyd S, Cross H, Baldeweg T. A possible role for gap junctions in generation of very fast EEG oscillations preceding the onset of, and perhaps initiating, seizures. *Epilepsia*. 2001; 42:153–170. [PubMed: 11240585]
- Traub RD, Cunningham MO, Gloveli T, LeBeau FEN, Bibbig A, Buhl EH, Whittington MA. GABA-enhanced collective behavior in neuronal axons underlies persistent gamma-frequency oscillations. *Proc Natl Acad Sci USA*. 2003; 100:11047–11052. [PubMed: 12960382]
- Traub RD, Contreras D, Cunningham MO, Murray H, LeBeau FEN, Roopun A, Bibbig A, Wilentz WB, Higley MJ, Whittington MA. Single-column thalamocortical network model exhibiting gamma oscillations, sleep spindles and epileptogenic bursts. *J Neurophysiol*. 2005; 93:2194–2232. [PubMed: 15525801]
- Traub RD, Duncan R, Russell AJC, Baldeweg T, Tu Y, Cunningham MO, Whittington MA. Spatiotemporal patterns of electrocorticographic very fast oscillations (>80 Hz) consistent with a network model based on electrical coupling between principal neurons. *Epilepsia*. 2010; 51:1587–1597. [PubMed: 20002152]
- Vladimirov N, Traub RD, Tu Y. Wave speed in excitable random networks with spatially constrained connections. *PLoS One*. 2011; 6:e20536. [PubMed: 21674028]
- Wang Y, Barakat A, Zhou H. Electrotonic coupling between pyramidal neurons in the neocortex. *PLoS One*. 2010; 5:e10253. [PubMed: 20436674]
- Worrell GA, Parish L, Cranston SD, Jonas R, Baltuch G, Litt B. High-frequency oscillations and seizure generation in neocortical epilepsy. *Brain*. 2004; 127:1496–1506. [PubMed: 15155522]

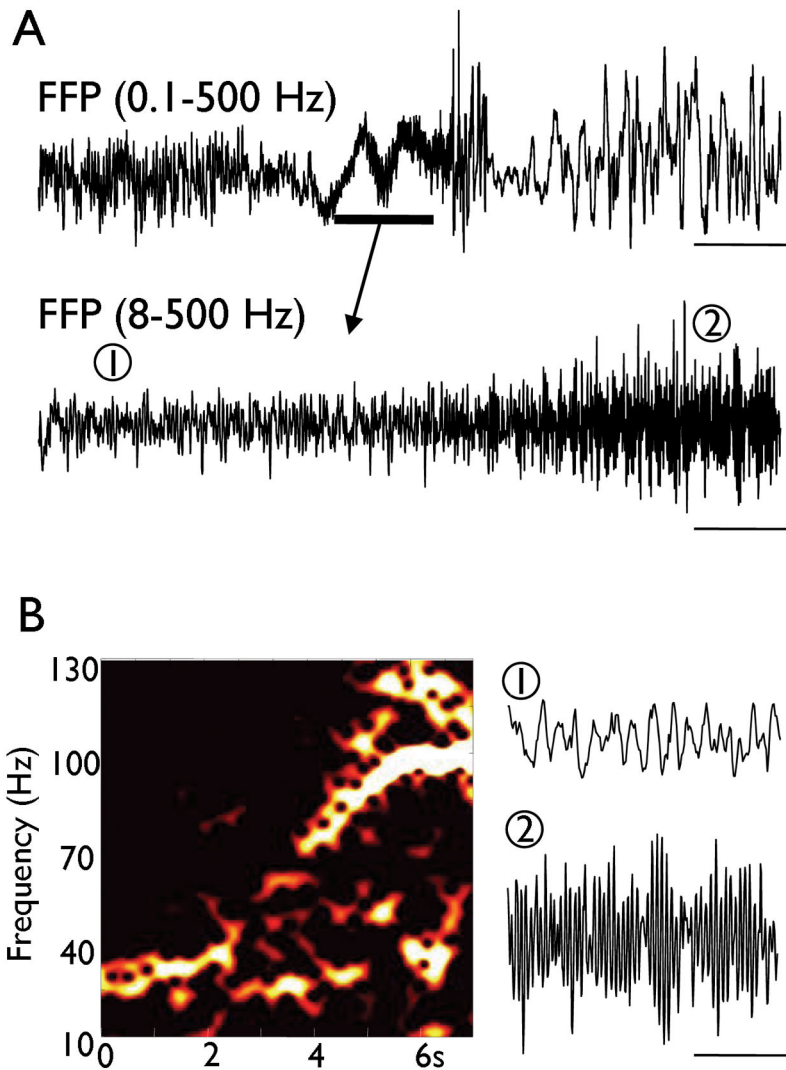


Figure 1. Glissando activity in pre-seizure ECoG recording (subdural grid), from a patient with seizures originating in temporal neocortex
 The patient is the same as described as patient B in Roopun et al. (2009). **A.** Example trace showing transition from normal ECoG activity to ictal event (upper). Note the appearance of large slow baseline fluctuations prior to full ictal discharge onset. A glissando discharge is revealed by removal of the slow baseline fluctuation with a higher pass band filter (lower trace). Scale bars 100 μ V, 5s, upper trace; 15 μ V, 0.8s, lower trace. **B.** Sliding window spectrogram (100 ms window width, offset 5 ms) illustrates the glissando occurring from 1 – 5 s into the lower trace shown in **A.** Example epochs of ECoG data are shown at the beginning (1) and end (2) of the event. Scale bars 15 μ V, 100 ms.

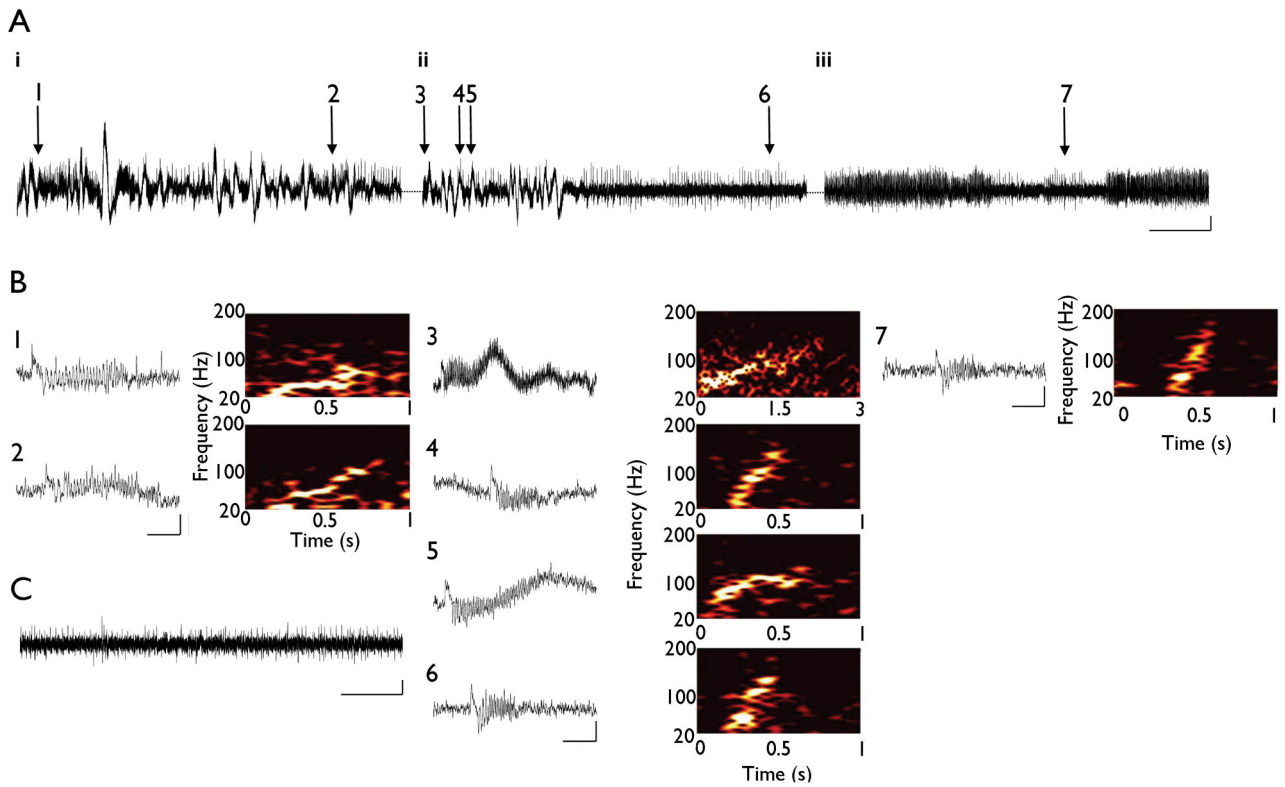


Figure 2. Association of multiple forms of glissando discharges in epileptic human neocortex with ictal behavior

A. Epileptic human temporal cortex slices obtained from patient 2 maintained in normal aCSF. Consecutive 60 s traces illustrate the onset of an ictal event (iii) preceded by slow DC potentials (i, ii) *in vitro*. Individual glissandi are indicated by numbered arrows. Scale bars 10 s, 1 mV **B.** Individual glissandi show a variety of temporal features. Expanded trace of each individual event highlighted in 'B' and the corresponding spectrogram shown to the right of the trace. Scale bars 0.2 s, 1 mV. **C.** 60 s trace of interictal sharp wave activity preceding the consecutive traces illustrates in 'A i–iii'. Scale bars 10 s, 1 mV. Note the increase in the occurrence of glissandi (ii) directly preceding the onset of the ictal discharge (iii).

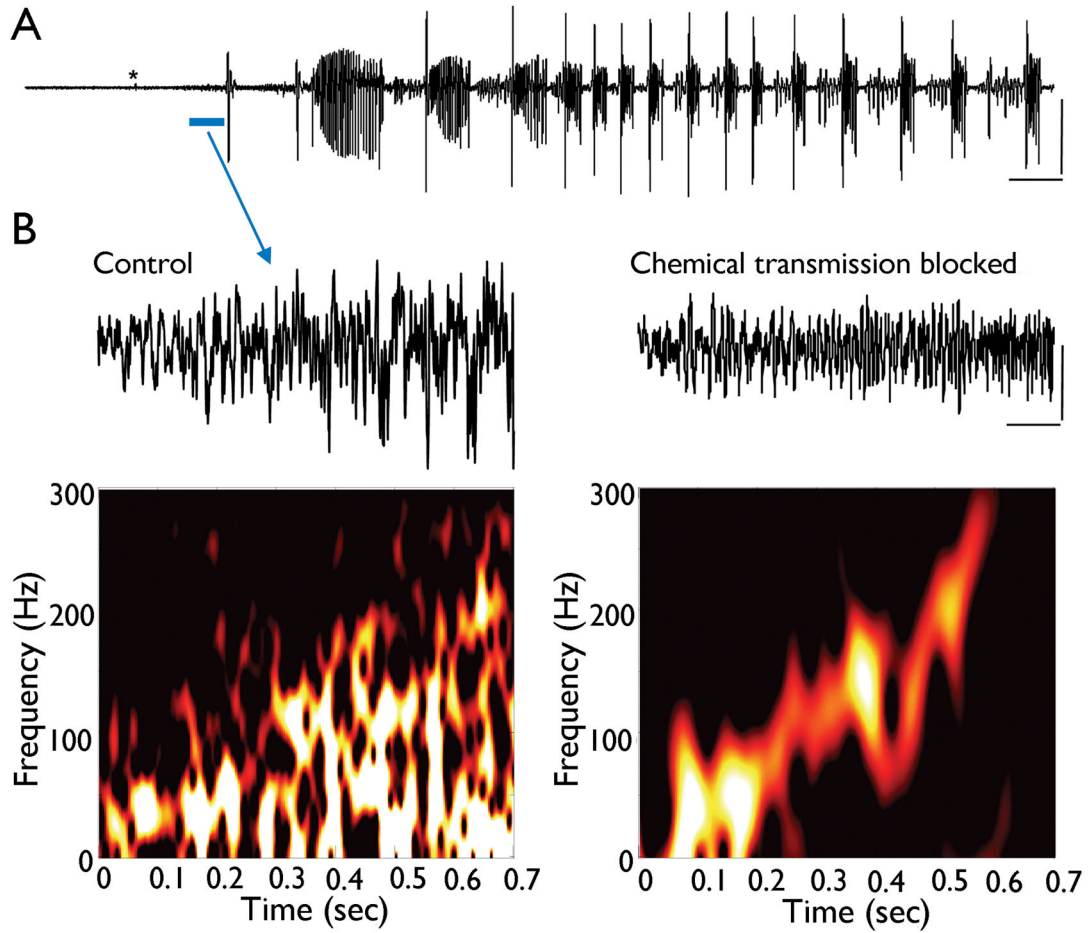


Figure 3. Experimental model of glissando discharges in normal rat neocortex: implication of pH
A. Rat frontal cortex maintained in normal ACSF. Transient alkalinization was induced by pressure ejection of 30–70 nl ACSF containing 200 mM NaOH (asterisk). This induced a gradual increase in low amplitude spontaneous activity with an increasing peak frequency until onset of ictal event lasting >30s. Scale bars 1 s, 2 mV. **B.** Comparison of glissando discharges evoked in normal conditions and conditions with the main chemical synaptic components blocked (gabazine, CGP55845, NBQX and D-AP5). The left trace is expanded from ‘A’ and the corresponding spectrogram shown below. The right trace shows response to the same alkalinizing ACSF pulse in the cocktail described above. Note: no ictiform events were seen with the chemical synaptic blockers present; and there is an absence of accompanying slower frequencies as the glissando progresses during blockade of chemical synapses. Scale bars 0.1 mV, 100 ms.

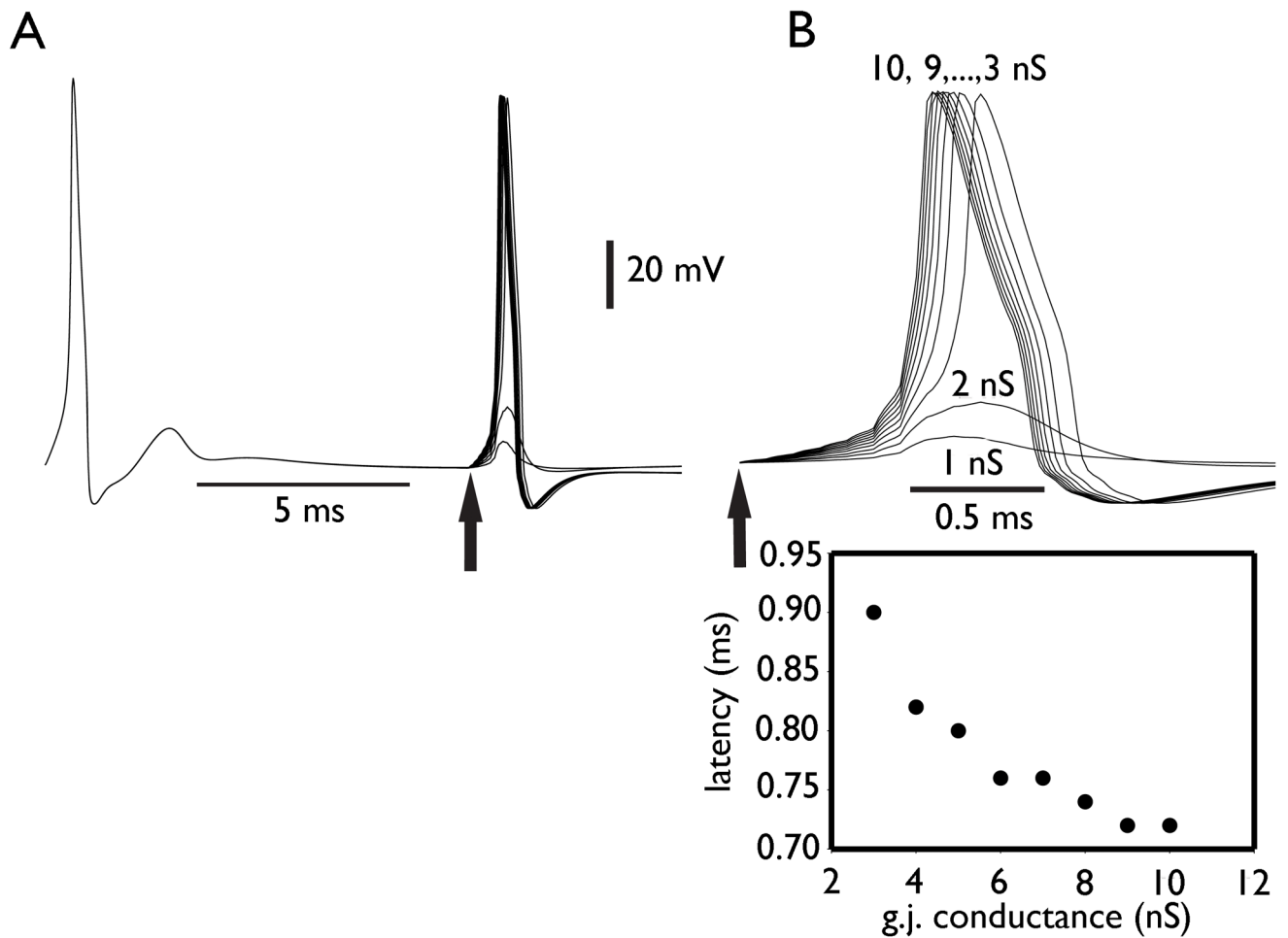


Figure 4. The latency for a spike to cross from axon to axon is predicted to decrease as gap junction conductance increases

Simulations of a single layer V pyramidal neuron, with a standardized prejunctional axonal spike coupled to an axonal compartment, through a conductance set at 1, 2, 3, ..., 10 nS. A: the superimposed traces of axonal potential, with the onset of the prejunctional spike at the time marked by the vertical arrow. B: details of the axonal potential. The threshold gap junction conductance for spike transmission was between 2 and 3 nS. With conductances above 3 nS, the latency for axonal spiking decreases, although with “diminishing returns”. The largest decrease occurs between 3 and 4 nS.

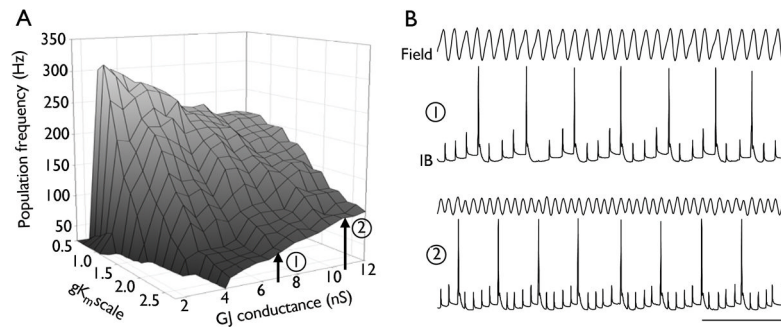


Figure 5. Parameter dependence of network frequency in model

A. Phase plot of field oscillation frequency, as a function of M-conductance ($g_{K(M)}$) and axonal gap junction conductance, based on simulations of a network of 15,000 model layer V pyramidal neurons coupled by axonal gap junctions. The model predicts that a “glissando” will occur if $g_{K(M)}$ is large enough, and gap junction conductance rises progressively. Network behavior is more complicated when $g_{K(M)}$ is small, with beta2 (~25 Hz) oscillations predicted to occur at small gap junction conductances (Roopun et al., 2006), with a rapid ‘switch’ to VFO with small increases in this parameter. **B.** Field and intracellular behavior, 400 ms epochs, at two values of gap junction conductance and fixed large $g_{K(M)}$ (scaling factor 2.7, corresponding to points 1 and 2 in Figure 5A). Note the increase in both field frequency and spikelet frequency, as gap junction conductance rises, for large enough M-conductance. Scale bars 100 ms, 50 mV (units for the fields are arbitrary, but the relative amplitudes are correct).

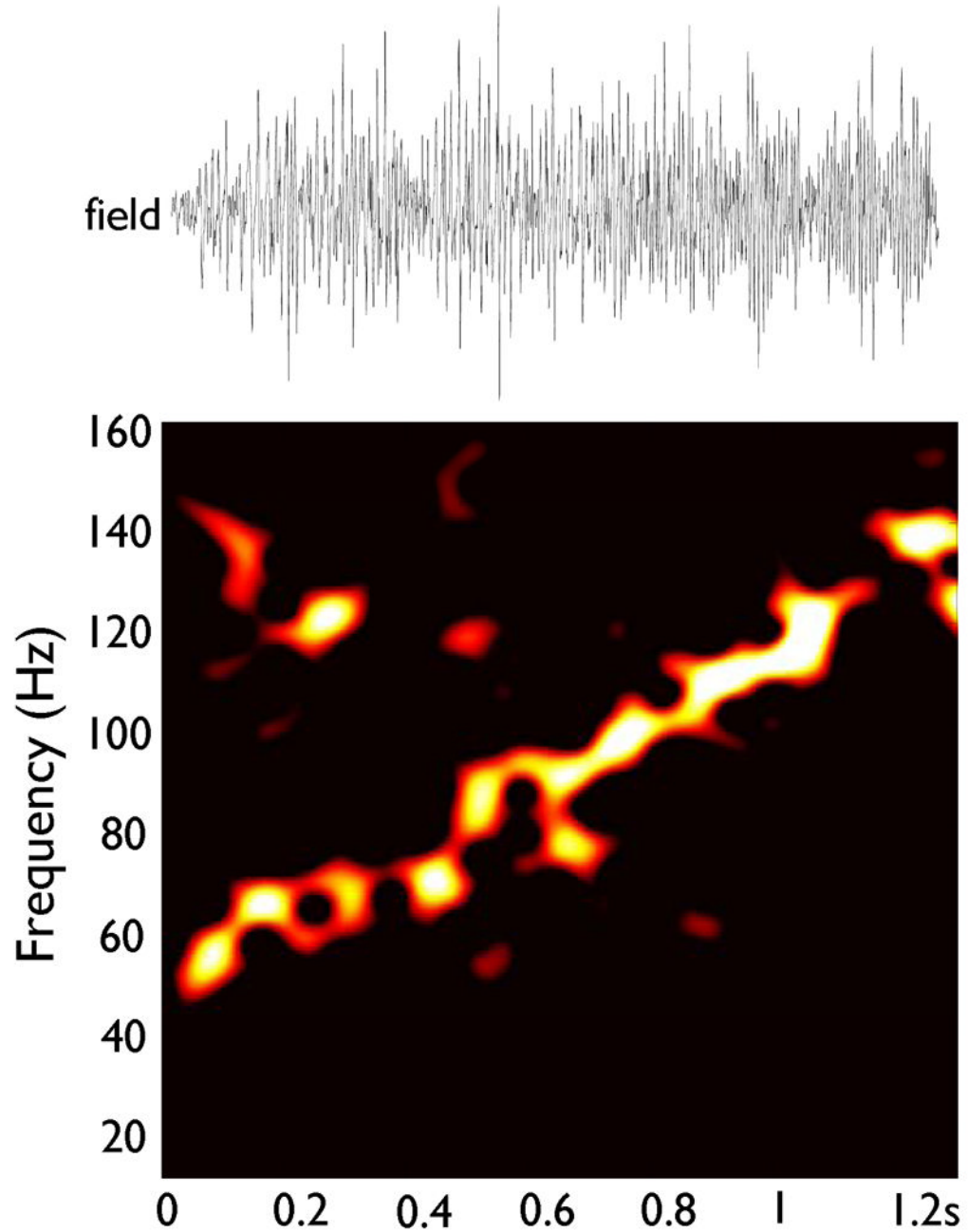


Figure 6. Glissando simulated by steadily rising gap junction conductance, in a network without chemical synapses

The network of Figure 5 was used ($g_{K(M)}$ scaling factor 2.7, as in Figure 5B); but axonal gap junction conductance rose progressively from 2.0 nS to 12.0 nS over a time interval of 2 seconds. Field amplitude is arbitrary, and field time scale is identical to the scale in the spectrogram below. Note the similarity to Figures 1B and 3B.